

000 001 002 003 004 005 006 007 008 009 010 GMTRouter: Personalized LLM Router over 011 012 013 014 015 016 017 018 019 020 021 022 023 024 025 026 027 028 Multi-Turn User Interactions

005 **Anonymous authors**

006 Paper under double-blind review

009 ABSTRACT

011 Large Language Model (LLM) routing has demonstrated strong capability in bal-
012 ancing response quality with computational cost. As users exhibit diverse pref-
013 erences, personalization has attracted increasing attention in LLM routing, since
014 even identical queries may require different models to generate responses tailored
015 to individual needs. However, existing approaches are not fully personalized and
016 often fail to faithfully capture the complex interactions between specific users
017 and LLMs. Moreover, user preference data is typically scarce, noisy, and inconsis-
018 tent in format, which limits the effectiveness of methods that rely solely on
019 user-specific data. To address these challenges, we propose *GMTRouter*, which
020 represents multi-turn user-LLM interactions as a heterogeneous graph with four
021 node types: user, LLM, query, and response, thereby maximally preserving the
022 rich relational structure of the interaction. Through a tailored message-passing
023 mechanism, *GMTRouter* learns to capture user preferences from few-shot data
024 within a lightweight inductive graph learning framework, enabling effective per-
025 sonalization. Extensive experiments demonstrate that *GMTRouter* consistently
026 outperforms the strongest baselines, achieving 0.9%–21.6% higher accuracy and
027 0.006–0.309 higher AUC across multiple datasets. More importantly, we further
028 demonstrate that *GMTRouter* can adapt to new users and evolving preferences
029 using only few-shot data, without extensive fine-tuning.

030 1 INTRODUCTION

031 With the rapid development of the field of Large Language Models (LLMs), an increasing number
032 of models with varying sizes, computational costs, and domain expertise have become available
033 (Singhal et al., 2023; Luo et al., 2022). This makes LLM routing particularly important, as it enables
034 the recommendation of appropriate LLMs for diverse user queries while balancing response quality
035 with computational cost (Šakota et al., 2024; Stripelis et al., 2024). Such routing techniques are
036 increasingly adopted in modern LLMs, including GPT-5 (OpenAI, 2025). At the same time, as more
037 users engage with LLM routing services, differences in individual preferences become increasingly
038 prominent: even identical queries may require different models to generate responses tailored to
039 each user (Li et al., 2024b; Salehi et al., 2024). Therefore, this paper aims to highlight a pressing
040 research question: *Can we design a personalized routing framework that aligns LLM selection with
041 individual user preferences based on their interaction histories?*

042 Existing research has proposed various architectures for LLM routing frameworks: FrugalGPT in-
043 troduces a BERT-based router that determines whether to switch to a larger LLM (Chen et al., 2023),
044 while C2MAB-V constructs a bandit-based router to balance exploration and exploitation when se-
045 lecting an LLM (Dai et al., 2024). GraphRouter formulates routing as a node classification task over
046 a graph of queries, tasks, and LLMs (Feng et al., 2024). However, existing methods largely overlook
047 the importance of extracting structured preference information from users’ interaction histories: they
048 are not fully personalized and often fail to faithfully model multi-turn conversations between users
049 and LLMs, which represent the most common form of user-LLM interaction in real-world scenar-
050 ios (Zhang et al., 2025a; Li et al., 2025b). Moreover, in real-world scenarios, the preference data
051 provided by a single user is typically scarce, noisy, and inconsistent in format (Escamocher et al.,
052 2024; Li et al., 2024a). This makes it challenging for methods that rely solely on user-specific data
053 to learn user profiles (Salemi et al., 2024a; Gao et al., 2024) or use such data as a retrieval source to
support routing (Au et al., 2025), thereby limiting their effectiveness.

054

Interaction History Table

User ID	Query	Selected LLM	Response	Feedback
User 1	[Turn 1]"Please Explain ... ?" [Turn 2]"Can a Process ... ?"	GPT-4-1106-Preview	[Turn 1]"Exothermic and endothermic ..." [Turn 2]"Yes, a process ..."	[Turn 1]"rating: 3.0" [Turn 2]"rating: 4.5"
User 2	[Turn 1]"Compose a blog ..."	Claude-V1	[Turn 1]"Title: Aloha Spirit ..."	[Turn 1]"ranking: Claude-V1 > Koala-13B"
User 2	[Turn 1]"Compose a blog ..."	Koala-13B	[Turn 1]"Aloha, fellow travelers ! ..."	[Turn 1]"ranking: Claude-V1 > Koala-13B"
User 3	[Turn 1]"Compose an email ..." [Turn 2]"Rewrite your"	Vicuna-13B	[Turn 1]"Subject: An Exciting ..." [Turn 2]"Subject: A Gental ..."	[Turn 1]"response: Subject: Embrace ..." [Turn 2]"response: Subject: Soaring to"

055

056

057

058

059

060

061

062

063

064

Figure 1: **Multi-turn user-LLM Interaction History Table.** Each row captures a multi-turn interaction with associated user feedback. User feedback can take various forms, including ratings, rankings, and ground-truth responses.

065

066

067

068

069

To address these challenges, we introduce **GMTRouter** (Graph Multi-Turn Router), a heterogeneous graph-based LLM router based on multi-turn user interactions for personalized LLM routing. GMTRouter first sensitively identifies key entities within the user-LLM interaction process: users, LLMs, queries, and responses. By modeling these entities as different types of nodes and encoding their textual information into node embeddings, it maximally preserves the semantic information from the original data. To faithfully model the relational structure of multi-turn user-LLM interactions, GMTRouter organizes these diverse node types into a heterogeneous graph that captures complex relational dependencies. Each single-turn interaction is treated as a fundamental unit, and a virtual node, referred to as a *turn node*, is introduced to aggregate local information within each interaction round. We further transform user preference feedback into node features, enabling preference information to propagate across the graph. Moreover, rather than training the model to directly extract specific user profiles from large historical datasets, GMTRouter employs a novel inductive graph training framework to **enhance the model’s ability to capture user preferences from few-shot data**. This design allows effective test-time personalization even under sparse interaction histories, such as cold-start scenarios involving new users. In summary, our main contributions are as follows:

085

086

087

088

089

090

091

092

093

094

095

096

097

- To the best of our knowledge, we are among the first to introduce an personalized LLM routing task based on multi-turn user interactions, providing new insights for this rapidly growing research field.
- We propose a novel personalized LLM routing framework, which faithfully models multi-turn user-LLM interactions as a heterogeneous graph, and learns to capture user preferences from few-shot data within a lightweight inductive graph learning framework.
- Through experiments on four datasets spanning diverse tasks, GMTRouter consistently outperforms the strongest baselines, achieving 0.9%–21.6% higher accuracy and 0.006–0.309 higher AUC. Moreover, we demonstrate that our method can efficiently adapt to unseen users with only a few interaction examples, without requiring retraining.

098

099

2 PRELIMINARIES

100

We introduce the personalized LLM routing task in this section. We focus on the multi-turn interaction scenario between users and LLMs with feedback (Wang et al., 2023b; Shi et al., 2024). Within a dialogue session, a user repeatedly interacts with a LLM: in each turn, the user issues a query, the LLM provides a response, and the user in turn supplies a piece of feedback. Such feedback can take multiple forms, including: (1) scalar scores (e.g., numerical ratings), (Wang et al., 2023c; 2024b); (2) preference rankings (e.g., choosing among multiple responses), (Yang et al., 2024; Sun et al., 2025); (3) ground-truth responses (e.g., directly providing the correct answer) (Gao et al., 2024; Salemi et al., 2024a). We structure these interactions into an **Interaction History Table**, illustrated in Figure 1, where each entry records the user ID, the selected LLM, the multi-turn queries and

108
 109
 110
 111
 112 Table 1: **The consistency of LLM preferences between users is significantly lower than the**
113 consistency within a single user’s preferences. The self-spearman score is substantially higher

114 than the spearman scores computed across different users.
 115
 116
 117 generated responses, and the corresponding user feedback, thereby maximally preserving the rich
 118 relational information of the interaction.
 119

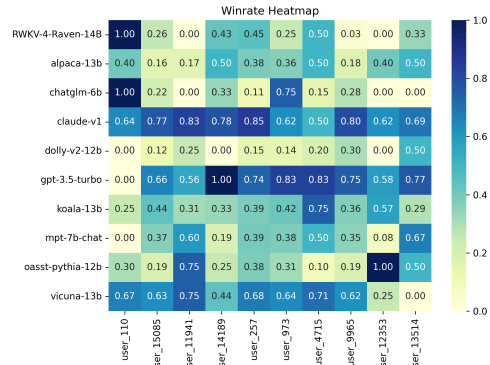
120 Our personalized LLM routing task is then modeled as follows: Given m users $\{u_1, \dots, u_m\}$ and n
 121 LLM candidates $\{m_1, \dots, m_n\}$, as well as their historical interaction records:
 122
 123

$$\mathcal{H} = \{(u_i, m_i, \{(q^{(t)}, r^{(t)}, f^{(t)})\}_{t=1}^{T_i})\},$$

124 where u_i is the user, m_i is the selected LLM, and each record contains a multi-turn sequence of
 125 queries $q^{(t)}$, responses $r^{(t)}$, and feedback $f^{(t)}$ for $t = 1, \dots, T_i$. When a user u raises a new query
 126 q , the router is required to select an LLM $m \in \{m_1, \dots, m_n\}$ to generate a response r that best
 127 aligns with the user preferences, which is measured through the feedback f provided by the user.
 128

129 2.2 MOTIVATION

130 In this section, we highlight the significant differences
 131 in LLM preferences across users in the real
 132 world (Chevi et al., 2025; Wang et al., 2024a), em-
 133 phasizing the importance of personalized LLM rout-
 134 ing for enhancing user experience. We use the Chat-
 135 Bot Arena dataset (Chiang et al., 2024) to illustrate
 136 our findings, which contains extensive anonymized
 137 multi-turn conversations from numerous users, with
 138 pairwise human preference labels between various
 139 LLMs, enabling the study of real-world user–LLM
 140 interactions. From this dataset, we select 10 active
 141 users, each with at least 50 records, for detailed
 142 analysis. For each user, we randomly split their data
 143 into two halves and compute the win rates of each
 144 LLM within each half. We use Spearman corre-
 145 lation to quantify the consistency of preference rank-
 146 ings over LLMs (De Winter et al., 2016; Hauke &
 147 Kossowski, 2011). We then compute the Spearman
 148 correlation between the two halves to quantify their
 149 self-consistency in preferences over LLMs (Chevi
 150 et al., 2025; Jiang et al., 2025), reporting the average
 151 as a baseline for comparison with inter-user prefer-
 152 ence consistency. Next, based on the similarity of queries in each user’s interaction history, we
 153 cluster users into three groups (Zeng et al., 2024; Li et al., 2025a), and compute pairwise Spear-
 154 man correlation scores among users globally, within clusters, and across clusters (Cavallo, 2019;
 155 De Winter et al., 2016), reporting the corresponding averages as summarized in Table 1. We observe
 156 that global consistency in LLM preferences among users is substantially lower than individual self-
 157 consistency, reaching only 65.99% of the latter. Even within the same cluster, the Spearman score
 158 is only 72.28% of the self-consistency, highlighting the diversity of user preferences toward LLMs
 159 (Sun et al., 2025; Salemi et al., 2024a). To further visualize these differences, we select the 10 most
 160 frequently used models across these 10 users and present a win-rate heatmap in Figure 2, offering
 161 an intuitive depiction of the variability in user preferences. Therefore, to address the substantial
 162 inconsistency of LLM preferences across users, we propose **GMTRouter**, a framework that enables
 163 the personalized recommendation of suitable LLMs tailored to each user’s individual preferences.



164
 165
 166
 167
 168
 169
 170
 171
 172
 173
 174
 175
 176
 177
 178
 179
 180
 181
 182
 183
 184
 185
 186
 187
 188
 189
 190
 191
 192
 193
 194
 195
 196
 197
 198
 199
 200
 201
 202
 203
 204
 205
 206
 207
 208
 209
 210
 211
 212
 213
 214
 215
 216
 217
 218
 219
 220
 221
 222
 223
 224
 225
 226
 227
 228
 229
 230
 231
 232
 233
 234
 235
 236
 237
 238
 239
 240
 241
 242
 243
 244
 245
 246
 247
 248
 249
 250
 251
 252
 253
 254
 255
 256
 257
 258
 259
 260
 261
 262
 263
 264
 265
 266
 267
 268
 269
 270
 271
 272
 273
 274
 275
 276
 277
 278
 279
 280
 281
 282
 283
 284
 285
 286
 287
 288
 289
 290
 291
 292
 293
 294
 295
 296
 297
 298
 299
 300
 301
 302
 303
 304
 305
 306
 307
 308
 309
 310
 311
 312
 313
 314
 315
 316
 317
 318
 319
 320
 321
 322
 323
 324
 325
 326
 327
 328
 329
 330
 331
 332
 333
 334
 335
 336
 337
 338
 339
 340
 341
 342
 343
 344
 345
 346
 347
 348
 349
 350
 351
 352
 353
 354
 355
 356
 357
 358
 359
 360
 361
 362
 363
 364
 365
 366
 367
 368
 369
 370
 371
 372
 373
 374
 375
 376
 377
 378
 379
 380
 381
 382
 383
 384
 385
 386
 387
 388
 389
 390
 391
 392
 393
 394
 395
 396
 397
 398
 399
 400
 401
 402
 403
 404
 405
 406
 407
 408
 409
 410
 411
 412
 413
 414
 415
 416
 417
 418
 419
 420
 421
 422
 423
 424
 425
 426
 427
 428
 429
 430
 431
 432
 433
 434
 435
 436
 437
 438
 439
 440
 441
 442
 443
 444
 445
 446
 447
 448
 449
 450
 451
 452
 453
 454
 455
 456
 457
 458
 459
 460
 461
 462
 463
 464
 465
 466
 467
 468
 469
 470
 471
 472
 473
 474
 475
 476
 477
 478
 479
 480
 481
 482
 483
 484
 485
 486
 487
 488
 489
 490
 491
 492
 493
 494
 495
 496
 497
 498
 499
 500
 501
 502
 503
 504
 505
 506
 507
 508
 509
 510
 511
 512
 513
 514
 515
 516
 517
 518
 519
 520
 521
 522
 523
 524
 525
 526
 527
 528
 529
 530
 531
 532
 533
 534
 535
 536
 537
 538
 539
 540
 541
 542
 543
 544
 545
 546
 547
 548
 549
 550
 551
 552
 553
 554
 555
 556
 557
 558
 559
 560
 561
 562
 563
 564
 565
 566
 567
 568
 569
 570
 571
 572
 573
 574
 575
 576
 577
 578
 579
 580
 581
 582
 583
 584
 585
 586
 587
 588
 589
 590
 591
 592
 593
 594
 595
 596
 597
 598
 599
 600
 601
 602
 603
 604
 605
 606
 607
 608
 609
 610
 611
 612
 613
 614
 615
 616
 617
 618
 619
 620
 621
 622
 623
 624
 625
 626
 627
 628
 629
 630
 631
 632
 633
 634
 635
 636
 637
 638
 639
 640
 641
 642
 643
 644
 645
 646
 647
 648
 649
 650
 651
 652
 653
 654
 655
 656
 657
 658
 659
 660
 661
 662
 663
 664
 665
 666
 667
 668
 669
 670
 671
 672
 673
 674
 675
 676
 677
 678
 679
 680
 681
 682
 683
 684
 685
 686
 687
 688
 689
 690
 691
 692
 693
 694
 695
 696
 697
 698
 699
 700
 701
 702
 703
 704
 705
 706
 707
 708
 709
 710
 711
 712
 713
 714
 715
 716
 717
 718
 719
 720
 721
 722
 723
 724
 725
 726
 727
 728
 729
 730
 731
 732
 733
 734
 735
 736
 737
 738
 739
 740
 741
 742
 743
 744
 745
 746
 747
 748
 749
 750
 751
 752
 753
 754
 755
 756
 757
 758
 759
 760
 761
 762
 763
 764
 765
 766
 767
 768
 769
 770
 771
 772
 773
 774
 775
 776
 777
 778
 779
 780
 781
 782
 783
 784
 785
 786
 787
 788
 789
 790
 791
 792
 793
 794
 795
 796
 797
 798
 799
 800
 801
 802
 803
 804
 805
 806
 807
 808
 809
 810
 811
 812
 813
 814
 815
 816
 817
 818
 819
 820
 821
 822
 823
 824
 825
 826
 827
 828
 829
 830
 831
 832
 833
 834
 835
 836
 837
 838
 839
 840
 841
 842
 843
 844
 845
 846
 847
 848
 849
 850
 851
 852
 853
 854
 855
 856
 857
 858
 859
 860
 861
 862
 863
 864
 865
 866
 867
 868
 869
 870
 871
 872
 873
 874
 875
 876
 877
 878
 879
 880
 881
 882
 883
 884
 885
 886
 887
 888
 889
 890
 891
 892
 893
 894
 895
 896
 897
 898
 899
 900
 901
 902
 903
 904
 905
 906
 907
 908
 909
 910
 911
 912
 913
 914
 915
 916
 917
 918
 919
 920
 921
 922
 923
 924
 925
 926
 927
 928
 929
 930
 931
 932
 933
 934
 935
 936
 937
 938
 939
 940
 941
 942
 943
 944
 945
 946
 947
 948
 949
 950
 951
 952
 953
 954
 955
 956
 957
 958
 959
 960
 961
 962
 963
 964
 965
 966
 967
 968
 969
 970
 971
 972
 973
 974
 975
 976
 977
 978
 979
 980
 981
 982
 983
 984
 985
 986
 987
 988
 989
 990
 991
 992
 993
 994
 995
 996
 997
 998
 999
 1000
 1001
 1002
 1003
 1004
 1005
 1006
 1007
 1008
 1009
 1010
 1011
 1012
 1013
 1014
 1015
 1016
 1017
 1018
 1019
 1020
 1021
 1022
 1023
 1024
 1025
 1026
 1027
 1028
 1029
 1030
 1031
 1032
 1033
 1034
 1035
 1036
 1037
 1038
 1039
 1040
 1041
 1042
 1043
 1044
 1045
 1046
 1047
 1048
 1049
 1050
 1051
 1052
 1053
 1054
 1055
 1056
 1057
 1058
 1059
 1060
 1061
 1062
 1063
 1064
 1065
 1066
 1067
 1068
 1069
 1070
 1071
 1072
 1073
 1074
 1075
 1076
 1077
 1078
 1079
 1080
 1081
 1082
 1083
 1084
 1085
 1086
 1087
 1088
 1089
 1090
 1091
 1092
 1093
 1094
 1095
 1096
 1097
 1098
 1099
 1100
 1101
 1102
 1103
 1104
 1105
 1106
 1107
 1108
 1109
 1110
 1111
 1112
 1113
 1114
 1115
 1116
 1117
 1118
 1119
 1120
 1121
 1122
 1123
 1124
 1125
 1126
 1127
 1128
 1129
 1130
 1131
 1132
 1133
 1134
 1135
 1136
 1137
 1138
 1139
 1140
 1141
 1142
 1143
 1144
 1145
 1146
 1147
 1148
 1149
 1150
 1151
 1152
 1153
 1154
 1155
 1156
 1157
 1158
 1159
 1160
 1161
 1162
 1163
 1164
 1165
 1166
 1167
 1168
 1169
 1170
 1171
 1172
 1173
 1174
 1175
 1176
 1177
 1178
 1179
 1180
 1181
 1182
 1183
 1184
 1185
 1186
 1187
 1188
 1189
 1190
 1191
 1192
 1193
 1194
 1195
 1196
 1197
 1198
 1199
 1200
 1201
 1202
 1203
 1204
 1205
 1206
 1207
 1208
 1209
 1210
 1211
 1212
 1213
 1214
 1215
 1216
 1217
 1218
 1219
 1220
 1221
 1222
 1223
 1224
 1225
 1226
 1227
 1228
 1229
 1230
 1231
 1232
 1233
 1234
 1235
 1236
 1237
 1238
 1239
 1240
 1241
 1242
 1243
 1244
 1245
 1246
 1247
 1248
 1249
 1250
 1251
 1252
 1253
 1254
 1255
 1256
 1257
 1258
 1259
 1260
 1261
 1262
 1263
 1264
 1265
 1266
 1267
 1268
 1269
 1270
 1271
 1272
 1273
 1274
 1275
 1276
 1277
 1278
 1279
 1280
 1281
 1282
 1283
 1284
 1285
 1286
 1287
 1288
 1289
 1290
 1291
 1292
 1293
 1294
 1295
 1296
 1297
 1298
 1299
 1300
 1301
 1302
 1303
 1304
 1305
 1306
 1307
 1308
 1309
 1310
 1311
 1312
 1313
 1314
 1315
 1316
 1317
 1318
 1319
 1320
 1321
 1322
 1323
 1324
 1325
 1326
 1327
 1328
 1329
 1330
 1331
 1332
 1333
 1334
 1335
 1336
 1337
 1338
 1339
 1340
 1341
 1342
 1343
 1344
 1345
 1346
 1347
 1348
 1349
 1350
 1351
 1352
 1353
 1354
 1355
 1356
 1357
 1358
 1359
 1360
 1361
 1362
 1363
 1364
 1365
 1366
 1367
 1368
 1369
 1370
 1371
 1372
 1373
 1374
 1375
 1376
 1377
 1378
 1379
 1380
 1381
 1382
 1383
 1384
 1385
 1386
 1387
 1388
 1389
 1390
 1391
 1392
 1393
 1394
 1395
 1396
 1397
 1398
 1399
 1400
 1401
 1402
 1403
 1404
 1405
 1406
 1407
 1408
 1409
 1410
 1411
 1412
 1413
 1414
 1415
 1416
 1417
 1418
 1419
 1420
 1421
 1422
 1423
 1424
 1425
 1426
 1427
 1428
 1429
 1430
 1431
 1432
 1433
 1434
 1435
 1436
 1437
 1438
 1439
 1440
 1441
 1442
 1443
 1444
 1445
 1446
 1447
 1448
 1449
 1450
 1451
 145

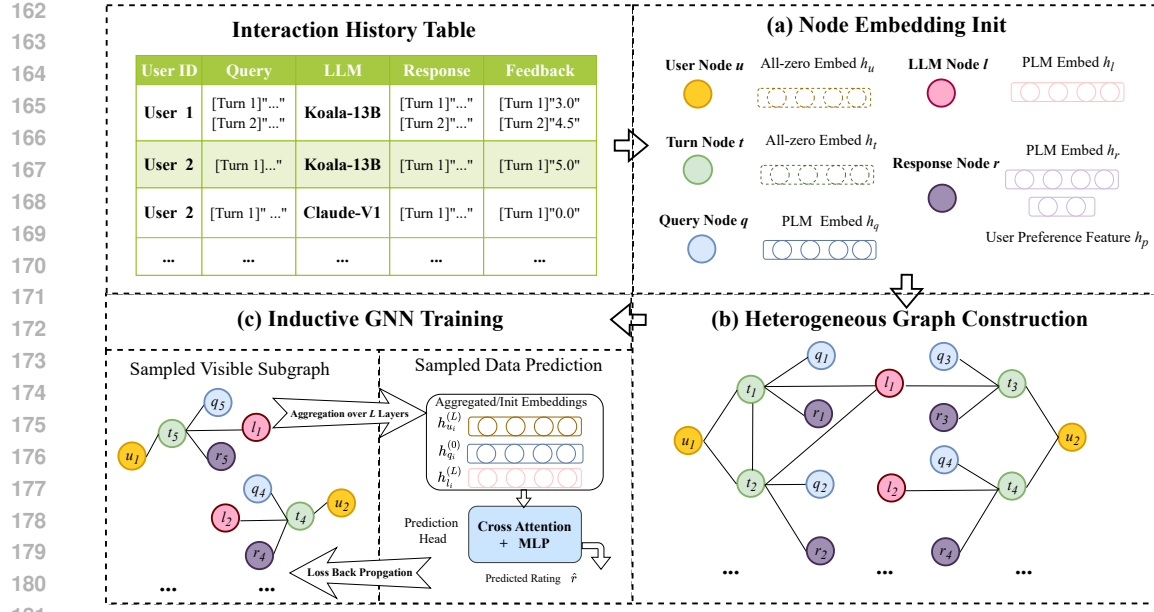


Figure 3: **Overview of GMTRouter.** (a) GMTRouter first extracts key entities: users, LLMs, queries, responses, and feedback, from the Interaction History Table and encodes their textual information using a PLM. (b) It then organizes these entities into a heterogeneous graph to faithfully model the relational structure of user–LLM interactions. (c) Within a lightweight inductive graph learning framework, GMTRouter learns to capture user preferences from few-shot data.

3 GMTROUTER: ROUTER OVER MULTI-TURN USER INTERACTIONS

Method Overview As shown in Figure 3, GMTROUTER operates in three stages: (a) It first identifies the key entities in the Interaction History Table—users, LLMs, queries, responses, and feedback—modeling them as nodes and encoding the textual information into node embeddings to maximally preserve the information of the interaction process. (b) Based on the relational structure of user–LLM interactions, these nodes are connected to form a heterogeneous graph, which captures rich relational dependencies. To facilitate information propagation, we further introduce a virtual *turn node* that aggregates the information within each single-round interaction. (c) Finally, we adopt a novel inductive graph training framework to learn how to capture user preferences from few-shot data, thereby enhancing the model’s ability to personalize under sparse user interaction histories.

3.1 NODE EMBEDDINGS INITIALIZATION.

First, our framework focuses on comprehensively extracting the information of various entities involved in the user–LLM interaction process from the Interaction History Table, along with their relational structures. As illustrated in part (a) of Figure 3, we extract four types of entities: user u , LLM m , query q , and response r , and formalize them as four corresponding node types. Their textual information is encoded using a pretrained language model (PLM) to obtain the initial node embeddings (Wang et al., 2022; 2023a), thereby preserving the semantic information from the original data. Specifically, we encode the query and response texts as their initial embeddings, denoted as h_q and h_r . In addition, we transform various forms of user feedback in the Interaction History Table into numerical ratings and project them into a User Preference Feature h_p , which serves as another attribute on the response nodes. Concretely, ranking feedback is discretized into numerical ratings to ensure that higher-ranked responses receive higher scores (Banditwattanawong & Masdisornchote, 2025); for ground-truth response feedback, we compute the geometric distance between the embeddings of the ground-truth and the generated response as the rating criterion (Salemi et al., 2024a). For LLM nodes, instead of simply using their names or IDs (Ding et al., 2024; Chen et al., 2023), we encode the model overviews provided by AI/ML API platforms¹ as their node embeddings h_m ,

¹<https://aimlapi.com/models/>

216 which typically include key information such as model size, usage cost, and domain-specific capabilities, thereby enriching the node embeddings with important background knowledge. Finally, for
 217 user nodes, we do not assume the existence of text-based user profiles, as such information is often
 218 scarce and noisy in real-world applications (Su et al., 2024; Alzubaidi et al., 2023); therefore, we
 219 initialize user embeddings h_u as zero vectors.
 220

222 3.2 HETEROGENEOUS GRAPH CONSTRUCTION.

224 Next, we organize these nodes into a heterogeneous graph to model the relational structure of
 225 user-LLM interactions (Zhang et al., 2025b; Schlichtkrull et al., 2017). We consider each single-
 226 round user-LLM interaction as a fundamental unit and introduce a kind of virtual node, *the turn*
 227 *node*, to aggregate the information within each interaction round. As illustrated in part (b) of Figure
 228 3, within each interaction round, the associated user node, LLM node, and generated query node,
 229 response node are all connected to the corresponding turn node, which serves to aggregate infor-
 230 mation from that round. For multi-turn conversations, the turn nodes corresponding to each round
 231 are sequentially connected in dialogue order, facilitating information propagation across turns. The
 232 turn node embedding h_t is initialized as zero vectors. The resulting heterogeneous graph captures
 233 the rich relational dependencies inherent in user-LLM interactions, where turn nodes aggregate lo-
 234 cal information within each dialogue round and propagate it to user nodes, thereby facilitating the
 235 global aggregation of user preference information.
 236

237 3.3 GNN AGGREGATION AND INDUCTIVE TRAINING

238 After constructing the user-LLM interaction histories into a heterogeneous graph, we train our GNN
 239 model on it. Notably, GMTRouter is a **general framework** that can incorporate any heterogeneous
 240 GNN as its backbone. We denote the GNN backbone used in our method as *GNN* throughout the
 241 rest of the paper.

242 To address scenarios with sparse user history (Su et al., 2024), instead of training the model to
 243 extract user profiles from large amounts of historical data (Lin et al., 2021; Wang et al., 2025),
 244 We employ an inductive framework along with **user-conditioned graph sampling** during training,
 245 enabling GMTRouter to capture a user’s preferences from only a few interaction records.
 246

247 **User-conditioned Graph Sampling** As illustrated in the left of (c) in Figure 3, during each training
 248 epoch, we sample k interaction histories for each user to construct a visible subgraph from the
 249 heterogeneous graph for message passing, and further sample data outside the visible subgraph as
 250 the prediction targets. We then use only these small sampled visible subgraphs and perform mes-
 251 sage aggregation separately for each user to update the node embeddings. Formally, at each layer l ,
 252 the embedding of a node v is updated by aggregating messages from its neighbors according to the
 253 message-passing mechanism of the backbone GNN:

$$254 \quad h_v^{(l)} = \text{Norm} \left(\text{Dropout} \left(\text{GNN}^{(l)}(h_v^{(l-1)}, \mathcal{G}_{\text{sub}}) \right) \right) \quad (1)$$

255 where $h_v^{(l)}$ denotes the embedding of node v at layer l , and \mathcal{G}_{sub} denotes the sampled visible sub-
 256 graph. $\text{Norm}(\cdot)$ denotes layer normalization, and $\text{Dropout}(\cdot)$ is applied for regularization.

257 This restriction on the amount of data involved in message passing encourages the model to learn
 258 how to infer user preferences from very limited signals and to generalize efficiently to new users.
 259

260 **LLM Routing with a Prediction Head.** After completing L layers of message aggregation, we
 261 obtain the updated node representations $h^{(L)}$. We then employ a **Prediction Head** module f_{pred}
 262 for preference prediction. As illustrated in the right of (c) in Figure 3, the Prediction Head takes
 263 the updated user embedding $h_u^{(L)}$, LLM embedding $h_m^{(L)}$, and the query embedding $h^{(0)}q$ from
 264 PLM as input. It applies a cross-attention module, where the LLM embedding attends to the fused
 265 user-query context to extract relevant preference signals. The module outputs a scalar score $s_{u,q,m}$
 266 for each LLM candidate, representing the likelihood that user u would prefer m to answer query:
 267

$$268 \quad s_{u,q,m} = f_{\text{pred}}(h_u^{(L)}, h_q^{(0)}, h_m^{(L)}) \quad (2)$$

270 These scores are then used to rank LLM candidates under the same (u, q) condition. We normalize
 271 both the predicted scores and the ground-truth ratings, and apply a criterion function to compute the
 272 training loss, which is subsequently used to update the model parameters.

273 During inference, when a user raises a new query, we first sample k interaction histories of that user
 274 to construct the visible subgraph and update the node embeddings. Then, the LLM candidate is
 275 selected from the candidate set \mathcal{M} as the one with the highest predicted score:

$$277 \quad m^* = \arg \max_{m \in \mathcal{M}} f_{\text{pred}}(h_u^{(L)}, h_q^{(0)}, h_m^{(L)}) \quad (3)$$

279 4 EXPERIMENT SETUP

281 4.1 DATASETS AND DATA PROCESSING

283 We conduct experiments on one real-world dataset and three additional synthetic datasets, covering
 284 four distinct tasks to enable a comprehensive evaluation of our approach.

- 286 • **Chatbot Arena (Chiang et al., 2024):** As mentioned in Section 2.2, we use the Chatbot Arena
 287 dataset to evaluate the personalized performance of our approach compared to baselines under
 288 authentic human preferences. For our experiments, we select the 11 users and 16 LLMs with the
 289 largest number of interactions. Detailed statistics are provided in Appendix B.1.
- 290 • **MT-Bench (Zheng et al., 2023):** MT-Bench is a benchmark for evaluating the reasoning and
 291 multi-turn conversational capabilities of LLMs, containing 80 multi-turn questions.
- 292 • **GSM8K (Cobbe et al., 2021):** GSM8K is a dataset of grade school-level math word problems,
 293 designed to assess LLMs’ mathematical reasoning and problem-solving skills.
- 294 • **MMLU (Hendrycks et al., 2021a;b):** MMLU is a comprehensive benchmark covering 57 sub-
 295 jects from professional domains, used to measure general knowledge and multi-domain reasoning
 296 abilities of LLMs. We sample 10 questions from each subject for our experiments.
- 297 • **LaMP (Salemi et al., 2024b):** LaMP is designed to evaluate language models across multiple
 298 dimensions of personalization. We select the “Personalized Scholarly Title Generation” task,
 299 which provides pairs of paper titles and abstracts for multiple users and requires predicting the
 300 title a user would prefer given an abstract. We convert this task into a personalized routing dataset,
 301 with processing details provided in Appendix B.3.

302 **Data Processing** For ChatBot Arena, we discretize the pairwise preferences to serve as the ratings
 303 for responses. For the other datasets, we adopt the data collected in Ong et al. (2024), which
 304 generated responses to all questions using “GPT-4-1106-preview” (Achiam et al., 2023) and “Mixtral-
 305 8x7B-Instruct-v0.1” (Jiang et al., 2024), and employed GPT-4 to provide quality annotations for
 306 open-ended questions. Based on this, we convert these datasets into multi-user personalized datasets.
 307 Specifically, for each response, we consider the following four dimensions: (a) Quality: For open-
 308 ended questions, we use the GPT-4 scores provided by Ong et al. (2024); for objective questions, we
 309 directly evaluate the correctness. (b) Cost: We calculate the cost of generating each response based
 310 on the API pricing provided by AI/ML API platform. (c) Response Length: We compute the token
 311 length of each response using the Contriever tokenizer (Izacard et al., 2021). (d) Rare Words: We
 312 count the number of rare words in each response using the *wordfreq* package (Speer, 2022).

313 We obtain the final rating of a response by computing a weighted sum of these four metrics. Different
 314 users are assigned different weightings to reflect their individual preferences over these dimensions
 315 (Feng et al., 2024; 2025). The specific weights used are provided in Appendix B.2.

316 **Data Splitting** For all datasets, we partition the data into training, validation, and test sets with
 317 a 7:1:2 ratio, ensuring that users are evenly distributed across the splits. For the GMTRouter, we
 318 further adopt an additional splitting strategy: we sample 30% of the users and restrict their data to
 319 the test sets only, in order to evaluate the generalization ability of our method to new users unseen
 320 during training.

322 4.2 BASELINES

323 We compare our GMTRouter against the following baselines:

324 **Prompt-based:** (1) **Vanilla LLM.** We incorporate the query and the descriptions of candidate LLMs
 325 into the prompt, and feed it into LLaMA-3.1-70B (Grattafiori et al., 2024) to select the LLM. (2)
 326 **Personalized LLM.** Building on the Vanilla LLM, we retrieve from the training set the ten inter-
 327 action histories most relevant to the user’s query and incorporate them into the prompt. Leveraging
 328 in-context learning Dong et al. (2022), the LLM is then guided to perform personalized routing.

329 **Representative Router:** (3) **GraphRouter.** (Feng et al., 2024) We adopt GraphRouter as the rep-
 330 resentative router baseline. It is a graph-based model that formulates routing as a node classification
 331 task over a graph of queries, tasks, and LLMs with learned edge interactions, and has shown superior
 332 performance over many existing routers (Ding et al., 2024; Chen et al., 2023; Dai et al., 2024) in
 333 non-personalized settings. (4) **FrugalGPT** (Chen et al., 2023) utilizes a PLM to predict the score
 334 of the generation result of all LLMs given a query, and then selects the LLM with the highest score
 335 within a given cost. (5) **RouteLLM** (Ong et al., 2024). Learns to route queries among a weak-
 336 strong pair of LLMs. Following the official setup, we designate the weak model as the one with the
 337 lower average win rate in the dataset, and the strong model as the one with the higher win rate.

338 **Sequential / memory-based recommender:** (6) **MA-GNN** (Chen Ma, 2020). A memory-
 339 augmented GNN that models both *short-term* and *long-term* user interests through item-level mes-
 340 sage passing and a dedicated memory module. We treat each user’s interaction history as a sequence
 341 of (query, LLM, feedback) records, where the sequential component captures short-term preference
 342 shifts and the memory module aggregates long-term preference signals; MA-GNN then predicts
 343 the preferred LLM for the current query. (7) **TIGER** (Shashank Rajput, 2023). A generative
 344 retrieval-based sequential recommender that models item sequences via semantic discrete codes;
 345 we regard LLMs as items and train TIGER to generate the semantic code of the best LLM condi-
 346 tioned on the user’s past interactions and current query, ranking candidate LLMs by their predicted
 347 likelihood.

348 4.3 METRICS

350 We evaluate the performance of all methods using two metrics:

- 352 • **Accuracy** measures how often the model correctly identifies the most preferred LLM to answer a
 given query from a specific user.
- 354 • **AUC-ROC** (Area Under the Receiver Operating Characteristic Curve) measures the model’s abil-
 355 ity to correctly rank candidate LLMs according to user preferences. We employ a pairwise ap-
 356 proach (C-index), defined as the probability that the predicted score s_+ for a preferred response
 357 (higher rating, r_+) is greater than the score s_- for a less preferred response (lower rating, r_-) over
 358 all comparable pairs: $AUC = \Pr(s_+ > s_-) + \frac{1}{2} \Pr(s_+ = s_-)$.

359 4.4 IMPLEMENTATION DETAILS

361 We implement our method using PyTorch Geometric (Fey & Lenssen, 2019) and conduct all exper-
 362 iments on a single NVIDIA RTX A6000 GPU. We employ Contriever (Izacard et al., 2021) as the
 363 PLM to obtain the initial node embeddings. We adopt the Heterogeneous Graph Transformer (HGT)
 364 (Ziniu Hu, 2020) as our model backbone due to its strong capability to maintain dedicated repres-
 365 entations for different types of nodes. Additionally, we experiment with various other heterogeneous
 366 GNNs as the backbone to investigate their impact on GMTRouter’s performance. Experimental de-
 367 tails are provided in Appendix F.4. We set the visible data size per user to $k = 10$ during both
 368 training and inference and adopt Entropy Loss as our loss function. In Section 5.2, we will experi-
 369 mentally analyze the impact of different values of k on our method, and hyperparameter details are
 370 provided in Appendix A.1.

371 5 EXPERIMENT RESULTS

372 5.1 COMPARISON WITH BASELINES

373 We compare GMTRouter with baselines across four datasets in Table 2. We observe that
 374 GMTRouter consistently outperforms all baselines, delivering an improvement of 0.9%–21.6% on
 375 accuracy and 0.006–0.309 on AUC compared to the strongest baselines, demonstrating the superior-

378 Table 2: **GMTRouter consistently outperforms baselines across all datasets.** Bold and under-
 379 line denote the best and second-best results. The results are averaged over multiple runs. Since
 380 RouteLLM and FrugalGPT are inherently binary routers, we evaluated them only in the binary set-
 381 ting from our datasets.

Method	Chatbot-Arena		MT-Bench		GSM8K		MMLU		LaMP	
	ACC	AUC	ACC	AUC	ACC	AUC	ACC	AUC	ACC	AUC
Vanilla LLM	0.525	0.741	0.481	0.457	0.546	0.533	0.473	0.475	-	-
Personalized LLM	0.646	0.780	0.437	0.491	0.553	0.536	0.675	0.678	0.312	0.605
GraphRouter	0.771	<u>0.869</u>	0.568	0.550	0.717	0.792	0.699	0.746	0.345	0.652
FrugalGPT	0.562	0.622	0.551	0.552	0.504	0.515	0.545	0.575	-	-
MA-GNN	0.673	0.775	0.679	0.739	0.636	0.648	0.702	0.758	<u>0.347</u>	0.661
TIGER	0.739	0.735	0.656	0.691	0.639	0.683	0.710	0.764	0.339	0.698
RouteLLM	0.492	0.485	0.480	0.475	0.499	0.498	0.532	0.513	-	-
Ours	<u>0.774</u>	0.875	0.784	0.859	0.773	0.859	0.771	0.870	0.349	<u>0.662</u>
Ours (new user)	0.780	0.858	<u>0.759</u>	0.824	0.756	0.833	<u>0.751</u>	0.831	-	-

393 Table 3: **GMTRouter requires only minimal storage and GPU resources.**

HGT Params	Pred Head Params	Total Params	Storage Overhead	Max GPU Usage
26.6M	0.85M	27.4M	109.6MB	4.3GB

399 ity of our framework. For Personalized LLM, although incorporating user interaction histories into
 400 prompts leads to improvements over Vanilla LLM on most datasets, it still lags behind GMTRouter
 401 by at least 9.6% in accuracy and 0.095 in AUC. This highlights the limited ability of LLMs to
 402 extract preference patterns from noisy user data. Moreover, our method consistently outperforms
 403 GraphRouter, a representative router that has shown strong performance in non-personalized LLM
 404 routing tasks, across all datasets. These results validate the importance of leveraging structured
 405 information from multi-turn user-LLM interaction data, together with user preference signals, to
 406 better align LLM selection with diverse user needs. Furthermore, even when 30% of users are not
 407 present in the training set, our method achieves performance comparable to the standard setting,
 408 underscoring its strong generalization ability to new users.

409 **Our Framework is Lightweight** We report the parameter count, storage overhead, and training
 410 resource requirements of GMTRouter in Table 3. With only 27.4M trainable parameters and a
 411 109.6MB model size, our framework remains compact compared to existing routing models. During
 412 training, only 4.3GB of GPU memory is needed, making it feasible to train on a single modern GPU
 413 without specialized hardware.

415 5.2 CASE STUDIES

417 **Investigating the Impact of Visible Data Size k** We investigate the impact of k visible data per
 418 user on the quality of the aggregated node embeddings. The results on GSM8K and MMLU are
 419 shown in Figure 4. As k increases, both accuracy and AUC improve, but beyond $k=10$, the perfor-
 420 mance begins to plateau or slightly decline, indicating diminishing returns from including additional
 421 visible data. This may be due to reduced generalization or potential instability caused by excessively
 422 large batch sizes during training (Keskar et al., 2016; Oyedotun et al., 2022). Therefore, we choose
 423 $k=10$ as a balanced setting for capturing user preferences without compromising generalization.

424 **Generalization to New Users** We further investigate the personalized capability of our method in
 425 few-shot scenarios with new users. Specifically, we evaluate on the GSM8K and MMLU by sam-
 426 pling 30% users from each dataset and varying the number of visible data $k \in \{3, 5, 8, 10, 15, 20\}$.
 427 Figure 5 presents averaged results of the sampled users under two settings: (i) the old user setting,
 428 where their records are included in the training set, and (ii) the new user setting, where they appear
 429 only in the validation and test sets. We observe that new users achieve results comparable to old
 430 users, and their performance curves consistently peak far above the GraphRouter baseline. These
 431 findings demonstrate that **our approach effectively learns to capture user preferences from few-
 432 shot data and can adapt to new users without requiring extensive fine-tuning.**

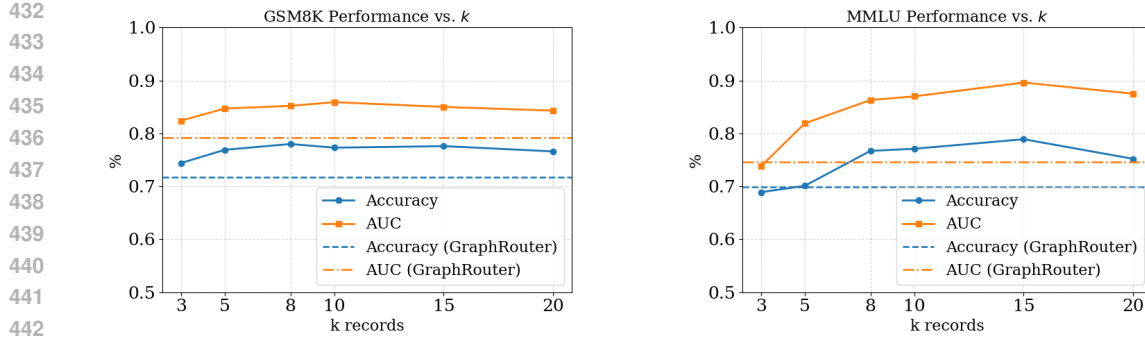


Figure 4: This figure illustrates **the impact of the visible data size k on GMTRouter for GSM8K (left) and MMLU (right)**. The dashed line represents the GraphRouter baseline. As k increases, the performance of our method improves, but it saturates once k reaches 10.

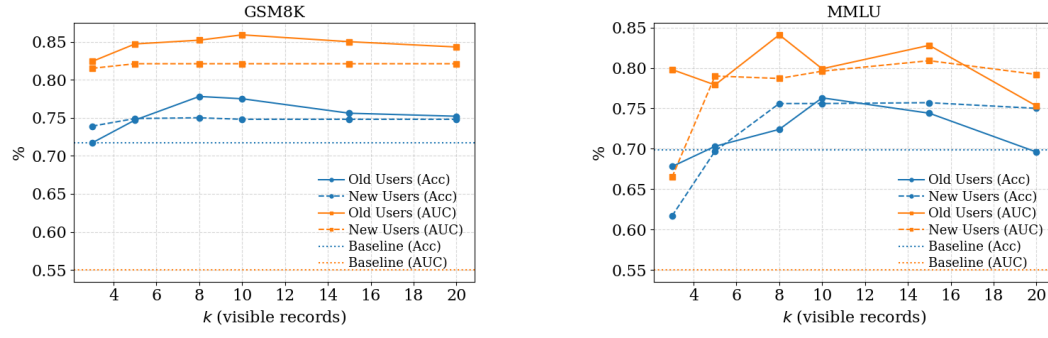


Figure 5: This figure illustrates the result comparison between old-user and new-user settings for GSM8K (left) and MMLU (right). The dashed line represents the GraphRouter baseline. The personalized performance under the new-user setting is comparable to that under the old-user setting, highlighting the strong generalization capability of our method.

5.3 ABLATION STUDIES

To evaluate the effectiveness of each design component of the GMTRouter, we conduct ablation studies along the following aspects.

- **w/o User Preference Feature** To verify the effectiveness of the user preference feature in propagating preference signals during GNN aggregation, we remove this feature in this variant. As a result, node embeddings are updated without incorporating preference ratings, which are used solely as supervision signals during training.
- **Dot-product Prediction Head** To evaluate whether the cross-attention prediction head captures non-linear interactions more effectively than standard similarity scoring when predicting the optimal model, we replace it in this variant with a simple dot product between the (user + query) and LLM embeddings.
- **Homogeneous Graph** To evaluate the effectiveness of our heterogeneous graph in capturing complex relationships among different entities in user-LLM interactions, we replace HGT with a homogeneous GNN, GraphSAGE (Hamilton et al., 2017), as the model backbone in this variant.
- **w/o User Embedding** To evaluate the effectiveness of user embeddings aggregated from the sampled visible graph for personalized prediction, we replace the user embeddings fed into the prediction head with zero vectors in this variant, thereby ablating their influence on the predictions.

The results of our ablation studies are presented in Table 4. As shown, our GMTRouter achieves the best performance on most metrics across all four datasets compared to the other variants, confirming the effectiveness of our design choices.

486 Table 4: **Ablation of design components.** We compare the full model with four variants: (1)
 487 removing the user preference features, (2) replacing the prediction head with a dot-product, (3)
 488 replacing HGT with GraphSAGE, (4) not using user embeddings during prediction. The best and
 489 second-best results are highlighted in **bold** and underline, respectively.

Method	Chatbot-Arena		MT-Bench		GSM8K		MMLU	
	Accuracy	AUC	Accuracy	AUC	Accuracy	AUC	Accuracy	AUC
w/o h_p	0.768	0.872	0.569	0.507	0.715	0.784	0.494	0.613
Dot-product	0.777	0.868	<u>0.730</u>	0.795	0.629	0.724	0.681	0.746
Homo Graph	0.768	<u>0.873</u>	0.569	0.645	0.635	0.648	0.494	0.487
w/o h_u	0.771	0.873	0.569	0.631	<u>0.725</u>	0.814	<u>0.701</u>	0.771
GMTRouter	<u>0.774</u>	0.875	0.784	0.859	0.773	0.859	0.771	0.870

6 ADDITIONAL RELATED WORKS

501 **LLM Routing.** LLM routing focuses on enhancing inference efficiency and response quality by
 502 assigning queries to the most appropriate model (Yue et al., 2025; Zhang et al., 2025c). Recent
 503 work frames routing as learning with cost-quality tradeoffs (Kadavath et al., 2022; Dekoninck et al.,
 504 2024); RouteLLM learns from preference data Ong et al. (2024), and RouterBench offers standard-
 505 ized routing benchmarks Hu et al. (2024). BEST-Route jointly selects LLM and generation count
 506 at test-time via a bandit controller Ding et al. (2025). However, existing approaches are not fully
 507 personalized and fail to exploit user information from interaction histories as well as the structure of
 508 multi-turn dialogues.

509 **Heterogeneous Graph Learning.** HetGNNs are designed to model heterogeneous graphs by cap-
 510 turing complex multi-type interactions among various nodes and edges (Chien et al., 2021; Feng
 511 et al., 2019). HAN uses hierarchical attention over metapaths Wang et al. (2019), while MAGNN
 512 and HeCo improve metapath aggregation and cross-view contrast Fu et al. (2020); Wang et al.
 513 (2021). Transformers such as HGT provide inductive, relation-aware message passing with tem-
 514 poral encoding Ziniu Hu (2020). This enables rich relational structures in user-LLM interactions
 515 while leveraging inductive training to enhance generalization on sparse data from new users.

516 **Personalized LLMs.** Personalized LLMs adapt a fixed base model rather than selecting among
 517 models. Memory-style methods extend long-term user/context memory (M+), combine episodic and
 518 semantic traces (PRIME), or tune user-specific knowledge graphs from feedback (KGT) (Yu Wang,
 519 2025; Xinliang Frederick Zhang, 2025; Jingwei Sun, 2024), while training-free patches port person-
 520 alization across evolving bases (PortLLM) (Rana Muhammad Shahroz Khan, 2025). By contrast, we
 521 study *personalized routing*—per-user selection among candidate LLMs from multi-turn histories.

7 CONCLUSION

525 In this work, we introduced GMTRouter, a heterogeneous graph-based framework for personalized
 526 LLM routing. By modeling multi-turn user-LLM interactions as a heterogeneous graph and prop-
 527 agating preference signals across node types, our method effectively captures user-specific patterns
 528 even from few-shot, noisy data. Experiments across four benchmarks confirm that GMTRouter con-
 529 sistently surpasses strong baselines in both accuracy and AUC, while adapting efficiently to new
 530 users without retraining. These results highlight the value of structured interaction modeling for
 531 advancing preference-aware LLM routing and point to promising future directions in scalable, user-
 532 aligned LLM deployment.

540 REFERENCES
541

542 Qwen2 technical report. 2024.

543 Josh Achiam, Steven Adler, Sandhini Agarwal, Lama Ahmad, Ilge Akkaya, Florencia Leoni Ale-
544 man, Diogo Almeida, Janko Altenschmidt, Sam Altman, Shyamal Anadkat, et al. Gpt-4 technical
545 report. *arXiv preprint arXiv:2303.08774*, 2023.546
547 AI@Meta. Llama 3 model card. 2024. URL https://github.com/meta-llama/llama3/blob/main/MODEL_CARD.md.548
549 Laith Alzubaidi, Jinshuai Bai, Aiman Al-Sabaawi, José I. Santamaría, A. Albahri, B. S. Al-dabbagh,
550 M. Fadhel, M. Manoufali, Jinglan Zhang, Ali H. Al-timemy, Ye Duan, Amjad Abdullah, Laith
551 Farhan, Yi Lu, Ashish Gupta, Felix Albu, Amin Abbosh, and Yuantong Gu. A survey on deep
552 learning tools dealing with data scarcity: definitions, challenges, solutions, tips, and applications.
553 *Journal of Big Data*, 10:1–82, 2023. doi: 10.1186/s40537-023-00727-2.554
555 Steven Au, Cameron J Dimacali, Ojasmitra Pedirappagari, Namyong Park, Franck Dernoncourt,
556 Yu Wang, Nikos Kanakaris, Hanieh Deilamsalehy, Ryan A Rossi, and Nesreen K Ahmed. Per-
557 sonalized graph-based retrieval for large language models. *arXiv preprint arXiv:2501.02157*,
558 2025.559
560 T. Banditwattanawong and Masawee Masdisornchote. Unbiased machine learning-assisted approach
561 for conditional discretization of human performances. *PeerJ Comput. Sci.*, 11:e2804, 2025. doi:
562 10.7717/peerj-cs.2804.563
564 B. Cavallo. Functional relations and spearman correlation between consistency indices. *Journal of
the Operational Research Society*, 71:301 – 311, 2019. doi: 10.1080/01605682.2018.1516178.565
566 Lingjiao Chen, Matei Zaharia, and James Zou. Frugalgpt: How to use large language models while
567 reducing cost and improving performance. *arXiv preprint arXiv:2305.05176*, 2023.568
569 Yingxue Zhang Jianing Sun Xue Liu Mark Coates Chen Ma, Liheng Ma. Memory augmented graph
570 neural networks for sequential recommendation. *AAAI 2020*, 2020.571
572 Rendi Chevi, Kentaro Inui, T. Solorio, and Alham Fikri Aji. How individual traits and lan-
573 guage styles shape preferences in open-ended user-llm interaction: A preliminary study. *ArXiv*,
abs/2504.17083, 2025. doi: 10.48550/arXiv.2504.17083.574
575 Wei-Lin Chiang, Lianmin Zheng, Ying Sheng, Anastasios Nikolas Angelopoulos, Tianle Li,
576 Dacheng Li, Hao Zhang, Banghua Zhu, Michael Jordan, Joseph Gonzalez, and Ion Stoica. Chat-
577 bot arena: An open platform for evaluating llms by human preference. *ArXiv*, abs/2403.04132,
2024. doi: 10.48550/arXiv.2403.04132.578
579 Eli Chien, Chao Pan, Jianhao Peng, and Olgica Milenkovic. You are allset: A multiset func-
580 tion framework for hypergraph neural networks. *arXiv preprint arXiv:2106.13264*, 2021. URL
581 <https://arxiv.org/abs/2106.13264>. ICLR 2022.582
583 Karl Cobbe, Vineet Kosaraju, Mohammad Bavarian, Mark Chen, Heewoo Jun, Lukasz Kaiser,
584 Matthias Plappert, Jerry Tworek, Jacob Hilton, Reiichiro Nakano, Christopher Hesse, and John
585 Schulman. Training verifiers to solve math word problems. *arXiv preprint arXiv:2110.14168*,
2021.586
587 Xiangxiang Dai, Jin Li, Xutong Liu, Anqi Yu, and John Lui. Cost-effective online multi-llm selec-
588 tion with versatile reward models. *arXiv preprint arXiv:2405.16587*, 2024.589
590 Joost CF De Winter, Samuel D Gosling, and Jeff Potter. Comparing the pearson and spearman
591 correlation coefficients across distributions and sample sizes: A tutorial using simulations and
592 empirical data. *Psychological methods*, 21(3):273, 2016.593 DeepSeek-AI. Deepseek-v3 technical report, 2024. URL <https://arxiv.org/abs/2412.19437>.

594 Jasper Dekoninck, Maximilian Baader, and Martin Vechev. A unified approach to routing and cas-
 595 cading for llms. *arXiv preprint arXiv:2410.10347*, 2024. URL <https://arxiv.org/abs/2410.10347>.

596

597 Dujian Ding, Ankur Mallick, Chi Wang, Robert Sim, Subhabrata Mukherjee, Victor Ruhle, Laks VS
 598 Lakshmanan, and Ahmed Hassan Awadallah. Hybrid llm: Cost-efficient and quality-aware query
 599 routing. *arXiv preprint arXiv:2404.14618*, 2024.

600

601 Dujian Ding, Ankur Mallick, Shaokun Zhang, Chi Wang, Daniel Madrigal, Mirian Del Car-
 602 men Hipolito Garcia, Menglin Xia, Laks V. S. Lakshmanan, Qingyun Wu, and Victor Rühle.
 603 Best-route: Adaptive llm routing with test-time optimal compute. In *Proceedings of the 42nd*
 604 *International Conference on Machine Learning (ICML)*, 2025. URL <https://arxiv.org/abs/2506.22716>. Also available as arXiv:2506.22716.

605

606 Qingxiu Dong, Lei Li, Damai Dai, Ce Zheng, Jingyuan Ma, Rui Li, Heming Xia, Jingjing Xu,
 607 Zhiyong Wu, Tianyu Liu, et al. A survey on in-context learning. *arXiv preprint arXiv:2301.00234*,
 608 2022.

609

610 Guillaume Escamocher, Samira Pourkhajouei, Federico Toffano, Paolo Viappiani, and Nic Wilson.
 611 Interactive preference elicitation under noisy preference models: An efficient non-bayesian ap-
 612 proach. *Int. J. Approx. Reason.*, 178:109333, 2024. doi: 10.1016/j.ijar.2024.109333.

613 Tao Feng, Yanzhen Shen, and Jiaxuan You. Graphrouter: A graph-based router for llm selections.
 614 *arXiv preprint arXiv:2410.03834*, 2024.

615

616 Tao Feng, Haozhen Zhang, Zijie Lei, Pengrui Han, Mostofa Patwary, Mohammad Shoeybi,
 617 Bryan Catanzaro, and Jiaxuan You. Fusing llm capabilities with routing data. *arXiv preprint*
 618 *arXiv:2507.10540*, 2025.

619

620 Yifan Feng, Haoxuan You, Zizhao Zhang, Rongrong Ji, and Yue Gao. Hypergraph neural networks.
 621 In *Proceedings of the AAAI Conference on Artificial Intelligence (AAAI)*, 2019. doi: 10.1609/aaai.v33i01.33013558. URL <https://ojs.aaai.org/index.php/AAAI/article/view/4235>.

622

623 Matthias Fey and Jan E. Lenssen. Fast graph representation learning with PyTorch Geometric. In
 624 *ICLR Workshop on Representation Learning on Graphs and Manifolds*, 2019.

625

626 Xinyu Fu, Jiani Zhang, Ziqiao Meng, and Irwin King. Magnn: Metapath aggregated graph neural
 627 network for heterogeneous graph embedding. In *Proceedings of The Web Conference (WWW)*,
 628 2020. doi: 10.1145/3366423.3380297. URL <https://dl.acm.org/doi/10.1145/3366423.3380297>.

629

630 Ge Gao, Alexey Taymanov, Eduardo Salinas, Paul Mineiro, and Dipendra Misra. Aligning llm
 631 agents by learning latent preference from user edits. *ArXiv*, abs/2404.15269, 2024. doi: 10.
 632 48550/arXiv.2404.15269.

633

634 Aaron Grattafiori, Abhimanyu Dubey, Abhinav Jauhri, Abhinav Pandey, Abhishek Kadian, Ahmad
 635 Al-Dahle, Aiesha Letman, Akhil Mathur, Alan Schelten, Alex Vaughan, et al. The llama 3 herd
 636 of models. *arXiv preprint arXiv:2407.21783*, 2024.

637

638 William L. Hamilton, Z. Ying, and J. Leskovec. Inductive representation learning on large graphs.
 639 *ArXiv*, abs/1706.02216, 2017.

640

641 Jan Hauke and Tomasz Kossowski. Comparison of values of pearson's and spearman's correlation
 642 coefficients on the same sets of data. *Quaestiones geographicae*, 30(2):87–93, 2011.

643

644 Dan Hendrycks, Collin Burns, Steven Basart, Andrew Critch, Jerry Li, Dawn Song, and Jacob
 645 Steinhardt. Aligning ai with shared human values. *Proceedings of the International Conference*
 646 *on Learning Representations (ICLR)*, 2021a.

647

648 Dan Hendrycks, Collin Burns, Steven Basart, Andy Zou, Mantas Mazeika, Dawn Song, and Jacob
 649 Steinhardt. Measuring massive multitask language understanding. *Proceedings of the Interna-*
 650 *tional Conference on Learning Representations (ICLR)*, 2021b.

648 Qijun Hu, Rui Zhang, Wenzuan Ren, Haoran Zhang, Minjia Zhang, Xinyu Zhou, Tong Liu, Pengfei
 649 Liu, Tong Zhang, and Mu Li. Routerbench: A benchmark for multi-llm routing system. *arXiv*
 650 *preprint arXiv:2403.12031*, 2024. URL <https://arxiv.org/abs/2403.12031>.

651 Gautier Izacard, Mathilde Caron, Lucas Hosseini, Sebastian Riedel, Piotr Bojanowski, Armand
 652 Joulin, and Edouard Grave. Unsupervised dense information retrieval with contrastive learning,
 653 2021. URL <https://arxiv.org/abs/2112.09118>.

654 Albert Q. Jiang, Alexandre Sablayrolles, Arthur Mensch, Chris Bamford, Devendra Singh Chap-
 655 lot, Diego de las Casas, Florian Bressand, Gianna Lengyel, Guillaume Lample, Lucile Saulnier,
 656 Lélio Renard Lavaud, Marie-Anne Lachaux, Pierre Stock, Teven Le Scao, Thibaut Lavril,
 657 Thomas Wang, Timothée Lacroix, and William El Sayed. Mistral 7b, 2023. URL <https://arxiv.org/abs/2310.06825>.

658 Albert Q. Jiang, Alexandre Sablayrolles, Antoine Roux, A. Mensch, Blanche Savary, Chris Bam-
 659 ford, Devendra Singh Chaplot, Diego de Las Casas, Emma Bou Hanna, Florian Bressand, Gi-
 660 anna Lengyel, Guillaume Bour, Guillaume Lample, L'elio Renard Lavaud, Lucile Saulnier,
 661 M. Lachaux, Pierre Stock, Sandeep Subramanian, Sophia Yang, Szymon Antoniak, Teven Le
 662 Scao, Théophile Gervet, Thibaut Lavril, Thomas Wang, Timothée Lacroix, and William El Sayed.
 663 Mixtral of experts. *ArXiv*, abs/2401.04088, 2024. doi: 10.48550/arXiv.2401.04088.

664 Bowen Jiang, Zhuoqun Hao, Young-Min Cho, Bryan Li, Yuan Yuan, Sihao Chen, Lyle Ungar, C. J.
 665 Taylor, and Dan Roth. Know me, respond to me: Benchmarking llms for dynamic user profiling
 666 and personalized responses at scale. *ArXiv*, abs/2504.14225, 2025. doi: 10.48550/arXiv.2504.
 667 14225.

668 Yiran Chen Jingwei Sun, Zhixu Du. Knowledge graph tuning: Real-time large language model
 669 personalization based on human feedback. [https://arxiv.org/pdf/2405.19686](https://arxiv.org/pdf/2405.19686.pdf), 2024.

670 Saurav Kadavath, Tom Conerly, Amanda Askell, Tom Henighan, Dawn Drain, Ethan Perez,
 671 Nicholas Schiefer, Zac Hatfield-Dodds, Nova DasSarma, Eli Tran-Johnson, et al. Language mod-
 672 els (mostly) know what they know. *arXiv preprint arXiv:2207.05221*, 2022. URL <https://arxiv.org/abs/2207.05221>.

673 N. Keskar, Dheevatsa Mudigere, J. Nocedal, M. Smelyanskiy, and P. T. P. Tang. On large-batch
 674 training for deep learning: Generalization gap and sharp minima. *ArXiv*, abs/1609.04836, 2016.

675 Haoxuan Li, Chunyuan Zheng, Wenjie Wang, Hao Wang, Fuli Feng, and Xiao-Hua Zhou. Debiased
 676 recommendation with noisy feedback. *Proceedings of the 30th ACM SIGKDD Conference on*
 677 *Knowledge Discovery and Data Mining*, 2024a. doi: 10.1145/3637528.3671915.

678 Xinyu Li, Z. Lipton, and Liu Leqi. Personalized language modeling from personalized human
 679 feedback. *ArXiv*, abs/2402.05133, 2024b. doi: 10.48550/arXiv.2402.05133.

680 Ying Li, Ye Zhong, Lijuan Yang, Yanbo Wang, and Penghua Zhu. Llm-guided crowdsourced test
 681 report clustering. *IEEE Access*, 13:24894–24904, 2025a. doi: 10.1109/ACCESS.2025.3530960.

682 Yubo Li, Xiaobin Shen, Xinyu Yao, Xueying Ding, Yidi Miao, R. Krishnan, and R. Padman.
 683 Beyond single-turn: A survey on multi-turn interactions with large language models. *ArXiv*,
 684 abs/2504.04717, 2025b. doi: 10.48550/arXiv.2504.04717.

685 Weiwei Lin, Hao Xu, Jianzhuo Li, Ziming Wu, Zhengyang Hu, Victor I. Chang, and J. Wang. Deep-
 686 profiling: a deep neural network model for scholarly web user profiling. *Cluster Computing*, 26:
 687 1753 – 1766, 2021. doi: 10.1007/s10586-021-03315-2.

688 Renqian Luo, Lliai Sun, Yingce Xia, Tao Qin, Sheng Zhang, Hoifung Poon, and Tie-Yan Liu. Biogpt:
 689 generative pre-trained transformer for biomedical text generation and mining. *Briefings in bioin-*
 690 *formatics*, 23(6):bbac409, 2022.

691 Isaac Ong, Amjad Almahairi, Vincent Wu, Wei-Lin Chiang, Tianhao Wu, Joseph E. Gonzalez, Mo-
 692 hammed Kadous, and Ion Stoica. Routellm: Learning to route llms with preference data. *arXiv*
 693 *preprint arXiv:2406.18665*, 2024. URL <https://arxiv.org/abs/2406.18665>.

702 OpenAI. Gpt-5 system card. Technical report, OpenAI, August 2025. URL <https://cdn.openai.com/gpt-5-system-card.pdf>.

703

704

705 O. Oyedotun, Konstantinos Papadopoulos, and D. Aouada. A new perspective for understanding
706 generalization gap of deep neural networks trained with large batch sizes. *Applied Intelligence*,
707 53:15621–15637, 2022. doi: 10.1007/s10489-022-04230-8.

708 Sukwon Yun Zhenyu Wang Shahriar Nirjon Chau-Wai Wong Tianlong Chen Rana Muhammad
709 Shahroz Khan, Pingzhi Li. Portllm: Personalizing evolving large language models with training-
710 free and portable model patches. *ICLR 2025*, 2025.

711

712 Marija Šakota, Maxime Peyrard, and Robert West. Fly-swat or cannon? cost-effective language
713 model choice via meta-modeling. In *Proceedings of the 17th ACM International Conference on*
714 *Web Search and Data Mining*, pp. 606–615, 2024.

715 Sogand Salehi, Mahdi Shafiei, Teresa Yeo, Roman Bachmann, and Amir Zamir. Viper: Visual
716 personalization of generative models via individual preference learning. pp. 391–406, 2024. doi:
717 10.48550/arXiv.2407.17365.

718

719 Alireza Salemi, Surya Kallumadi, and Hamed Zamani. Optimization methods for personalizing
720 large language models through retrieval augmentation. In *Proceedings of the 47th International*
721 *ACM SIGIR Conference on Research and Development in Information Retrieval*, pp. 752–762,
722 2024a.

723 Alireza Salemi, Sheshera Mysore, Michael Bendersky, and Hamed Zamani. Lamp: When large
724 language models meet personalization. In *Proceedings of the 62nd Annual Meeting of the Asso-*
725 *ciation for Computational Linguistics (Volume 1: Long Papers)*, pp. 7370–7392, 2024b.

726 M. Schlichtkrull, Thomas Kipf, Peter Bloem, Rianne van den Berg, Ivan Titov, and M. Welling.
727 Modeling relational data with graph convolutional networks. pp. 593–607, 2017. doi: 10.1007/
728 978-3-319-93417-4_38.

729

730 Anima Singh Raghunandan Hulikal Keshavan Trung Vu Lukasz Heldt-Lichan Hong Yi Tay
731 Vinh Tran Jonah Samost Maciej Kula Ed Chi Maheswaran Sathiamoorthy Shashank Rajput,
732 Nikhil Mehta. Recommender systems with generative retrieval. *NeurIPS 2023*, 2023.

733 Taiwei Shi, Zhuoer Wang, Longqi Yang, Ying-Chun Lin, Zexue He, Mengting Wan, Pei Zhou,
734 S. Jauhar, Xiaofeng Xu, Xia Song, and Jennifer Neville. Wildfeedback: Aligning llms with in-situ
735 user interactions and feedback. *ArXiv*, abs/2408.15549, 2024. doi: 10.48550/arXiv.2408.15549.

736

737 Karan Singhal, Shekoofeh Azizi, Tao Tu, S Sara Mahdavi, Jason Wei, Hyung Won Chung, Nathan
738 Scales, Ajay Tanwani, Heather Cole-Lewis, Stephen Pfahl, et al. Large language models encode
739 clinical knowledge. *Nature*, 620(7972):172–180, 2023.

740 Robyn Speer. rspeer/wordfreq: v3.0, September 2022. URL <https://doi.org/10.5281/zenodo.7199437>.

741

742

743 Dimitris Stripelis, Zijian Hu, Jipeng Zhang, Zhaozhuo Xu, Alay Shah, Han Jin, Yuhang Yao, Salman
744 Avestimehr, and Chaoyang He. Polyrouter: A multi-llm querying system. *arXiv e-prints*, pp.
745 arXiv–2408, 2024.

746 Hongzu Su, Jingjing Li, Zhekai Du, Lei Zhu, Ke Lu, and H. Shen. Cross-domain recommendation
747 via dual adversarial adaptation. *ACM Transactions on Information Systems*, 42:1 – 26, 2024. doi:
748 10.1145/3632524.

749

750 Yihang Sun, Tao Feng, Ge Liu, and Jiaxuan You. Premium: Llm personalization with individual-
751 level preference feedback. *ArXiv*, 2025.

752 Gemma Team. Gemma. 2024. doi: 10.34740/KAGGLE/M/3301. URL <https://www.kaggle.com/m/3301>.

753

754

755 Haifeng Wang, Jiwei Li, Hua Wu, Eduard Hovy, and Yu Sun. Pre-trained language models and their
applications. *Engineering*, 25:51–65, 2023a.

756 Haoxiang Wang, Yong Lin, Wei Xiong, Rui Yang, Shizhe Diao, Shuang Qiu, Han Zhao, and Tong
 757 Zhang. Arithmetic control of llms for diverse user preferences: Directional preference alignment
 758 with multi-objective rewards. pp. 8642–8655, 2024a. doi: 10.48550/arXiv.2402.18571.

759 Liang Wang, Nan Yang, Xiaolong Huang, Binxing Jiao, Linjun Yang, Dixin Jiang, Rangan Ma-
 760 jumder, and Furu Wei. Text embeddings by weakly-supervised contrastive pre-training. *arXiv*
 761 *preprint arXiv:2212.03533*, 2022.

762 Xiao Wang, Houye Ji, Chuan Shi, Bai Wang, Peng Cui, Philip S. Yu, and Yanfang Ye. Heterogeneous
 763 graph attention network. In *Proceedings of The Web Conference (WWW)*, 2019. URL <https://arxiv.org/abs/1903.07293>.

764 Xiao Wang, Xiangnan He, Yuesong Cao, Meng Liu, and Tat-Seng Chua. Self-supervised hetero-
 765 geneous graph neural network with co-contrastive learning. In *Proceedings of the 27th ACM*
 766 *SIGKDD Conference on Knowledge Discovery & Data Mining (KDD)*, 2021. doi: 10.1145/3447548.3467415. URL <https://dl.acm.org/doi/10.1145/3447548.3467415>.

767 Xingyao Wang, Zihan Wang, Jiateng Liu, Yangyi Chen, Lifan Yuan, Hao Peng, and Heng Ji.
 768 Mint: Evaluating llms in multi-turn interaction with tools and language feedback. *ArXiv*,
 769 [abs/2309.10691](https://arxiv.org/abs/2309.10691), 2023b. doi: 10.48550/arXiv.2309.10691.

770 Zhaoyang Wang, Li Li, Ketai He, and Zhenyang Zhu. User profile construction based on high-
 771 dimensional features extracted by stacking ensemble learning. *Applied Sciences*, 2025. doi:
 772 10.3390/app15031224.

773 Zhilin Wang, Yi Dong, Jiaqi Zeng, Virginia Adams, Makesh Narsimhan Sreedhar, Daniel Egert,
 774 Olivier Delalleau, Jane Polak Scowcroft, Neel Kant, Aidan Swope, et al. Helpsteer: Multi-
 775 attribute helpfulness dataset for steerlm. *arXiv preprint arXiv:2311.09528*, 2023c.

776 Zhilin Wang, Yi Dong, Olivier Delalleau, Jiaqi Zeng, Gerald Shen, Daniel Egert, Jimmy Zhang,
 777 Makesh Narsimhan Sreedhar, and Oleksii Kuchaiiev. Helpsteer2: Open-source dataset for training
 778 top-performing reward models. *ArXiv*, [abs/2406.08673](https://arxiv.org/abs/2406.08673), 2024b. doi: 10.48550/arXiv.2406.08673.

779 Lu Wang Xinliang Frederick Zhang, Nicholas Beauchamp. Prime: Large language model personal-
 780 ization with cognitive dual-memory and personalized thought process. *ACL*, 2025.

781 Hongyu Yang, Liyang He, Min Hou, Shuanghong Shen, Rui Li, Jiahui Hou, Jianhui Ma, and Junda
 782 Zhao. Aligning llms through multi-perspective user preference ranking-based feedback for pro-
 783 gramming question answering. *ArXiv*, [abs/2406.00037](https://arxiv.org/abs/2406.00037), 2024. doi: 10.48550/arXiv.2406.00037.

784 Yuanzhe Hu Yifan Gao Wangchunshu Zhou Julian McAuley Dan Gutfreund Rogerio Feris Zexue He
 785 Yu Wang, Dmitry Krotov. M+: Extending memoryllm with scalable long-term memory. *ICML*
 786 2025, 2025.

787 Yanwei Yue, Guibin Zhang, Boyang Liu, et al. Masrouter: Learning to route llms for multi-
 788 agent systems. In *Proceedings of the 63rd Annual Meeting of the ACL*, 2025. URL <https://aclanthology.org/2025.acl-long.757/>.

789 Hang Zeng, Chaoyue Niu, Fan Wu, Chengfei Lv, and Guihai Chen. Personalized llm for generating
 790 customized responses to the same query from different users. *ArXiv*, [abs/2412.11736](https://arxiv.org/abs/2412.11736), 2024. doi:
 791 10.48550/arXiv.2412.11736.

792 Chen Zhang, Xinyi Dai, Yaxiong Wu, Qu Yang, Yasheng Wang, Ruiming Tang, and Yong Liu. A
 793 survey on multi-turn interaction capabilities of large language models. *ArXiv*, [abs/2501.09959](https://arxiv.org/abs/2501.09959),
 794 2025a. doi: 10.48550/arXiv.2501.09959.

795 Chi Zhang, Junho Jeong, and Jin-Woo Jung. Anomaly detection over multi-relational graphs using
 796 graph structure learning and multi-scale meta-path graph aggregation. *IEEE Access*, 13:60303–
 797 60316, 2025b. doi: 10.1109/ACCESS.2025.3554407.

798 Yihan Zhang, Kai Wang, Zexuan Li, Wenqi Xu, Haoran Zhu, and Wei Chen. Mixllm: Dynamic rout-
 799 ing in mixed large language models. In *Proceedings of the 2025 Conference of the North Ameri-
 800 can Chapter of the ACL (NAACL)*, 2025c. URL <https://aclanthology.org/2025.naacl-long.545/>.

810 Lianmin Zheng, Wei-Lin Chiang, Ying Sheng, Siyuan Zhuang, Zhanghao Wu, Yonghao Zhuang,
811 Zi Lin, Zhuohan Li, Dacheng Li, Eric Xing, et al. Judging llm-as-a-judge with mt-bench and
812 chatbot arena. *Advances in neural information processing systems*, 36:46595–46623, 2023.

813
814 Kuansan Wang Yizhou Sun Ziniu Hu, Yuxiao Dong. Heterogeneous graph transformer. *WWW'20*,
815 2020.

816
817
818
819
820
821
822
823
824
825
826
827
828
829
830
831
832
833
834
835
836
837
838
839
840
841
842
843
844
845
846
847
848
849
850
851
852
853
854
855
856
857
858
859
860
861
862
863

864 **A IMPLEMENTATION DETAILS**

865

866 **A.1 MODEL CONFIGURATION AND HYPERPARAMETERS**

867

868 **Architecture.** We use a heterogeneous graph transformer (HGTran) with:

869

- **GNN:** 2 layers (single-turn) or 3 (multi-turn), 768-dim hidden, 4-head HGTranConv, Layer-Norm, dropout 0.1.
- **Predictor:** 4-head MLP with hidden dim 256, dropout 0.1; uses cross-attention where LLM attends to user+query.

870

871 **Training.**

872

- **Epochs:** 350 **LR:** 5e-4
- **Visible records/user (k):** {3, 5, 8, 10, 15, 20}
- **Batch size:** 256 supervision triplets
- **Ranking Objective:** prioritize AUC, then Accuracy

873

874 **A.2 TRAINING OF GMTRROUTER**

875

876 **Algorithm 1:** Training GMTRROUTER

877

878 **Data:** $\mathcal{D}_{\text{train}} = \{(x, y)\}$ 879 **Hyperparams:** epochs E , visible k , supervision s , PLM, GNN f_ϕ , predictor Pred 880 **Init:** PLM-encode all nodes; initialize node/edge features

881

```

1 for  $e \leftarrow 1$  to  $E$  do
2    $\mathcal{G}^{(e)} \leftarrow$  subgraph from  $k|\mathcal{U}|$  visible records
3    $\mathcal{M}^{(e)} \leftarrow s$  held-out triples  $(u, q, m)$ 
4    $h \leftarrow f_\phi(\mathcal{G}^{(e)})$  // message passing
5   for  $(u, q, m) \in \mathcal{M}^{(e)}$  do
6      $\hat{y} \leftarrow \text{Pred}(h_u, q, h_m)$ 
7   Update  $f_\phi$  and  $\text{Pred}$  by minimizing  $\mathcal{L}_{\text{rank}}(\hat{y}, y)$ 

```

882

883

884

885 **B DATASET PREPARATION**

886

887 **B.1 DATASET STATISTICS**

888

We preprocess each dataset by extracting user–query–LLM–response tuples and partition them into train, validation, and test sets. To ensure fair evaluation and meaningful personalization, we stratify the splits to maintain balanced user–model preference distributions and avoid degenerate cases (e.g., users consistently preferring a single LLM or lacking query diversity). This setup promotes generalization under cold-start conditions and supports robust evaluation of routing behavior.

889

For ChatBot Arena, we selected the following users and LLMs:

890

Users: arena_user_9965, arena_user_15085, arena_user_257, arena_user_13046, arena_user_11473, arena_user_3820, arena_user_9676, arena_user_6467, arena_user_6585, arena_user_5203, arena_user_1338

891

LLMs: koala-13b, vicuna-13b, gpt-3.5-turbo, oasst-pythia-12b, gpt-4, claude-v1, RWKV-4-Raven-14B, palm-2, alpaca-13b, mpt-7b-chat, vicuna-7b, claude-instant-v1, chatglm-6b, fastchat-t5-3b, dolly-v2-12b, stablelm-tuned-alpha-7b

892

We report in Table 6 the size of each dataset along with the time required to process it into the heterogeneous graph used in our experiments.

Table 5: Dataset statistics, including the number of entries, users, and LLMs in each split.

Dataset	Split	#Entries	#Users	#LLMs
Chatbot-Arena	Train	2780	11	16
	Valid	386	11	16
	Test	824	11	16
MT-Bench	Train	2240	10	2
	Valid	320	10	2
	Test	640	10	2
GSM8K	Train	18460	10	2
	Valid	2620	10	2
	Test	5300	10	2
MMLU	Train	3970	5	2
	Valid	560	5	2
	Test	1150	5	2

Table 6: Computational cost of graph construction across datasets.

Dataset	Data Entries	Avg. Tokens	Encoding Time (s)	Graph Construction Time (s)
ChatBot-Arena	3990	184.41	51.73	1.70
MT-Bench	3200	4511.73	55.68	2.40
GSM8K	26380	112.68	142.84	1.49
MMLU	5680	9.35	4.27	1.56
LaMP	9850	66.82	30.98	1.91

B.2 SYNTHETIC USER DESIGN

To simulate diverse user preferences, we introduce synthetic users whose routing behavior is governed by a weighted linear utility function over multiple metrics: human preference rating, token count, output diversity, and cost. For each dataset, we manually assign different weights $\{w_{\text{rating}}, w_{\text{tokens}}, w_{\text{diff}}, w_{\text{cost}}\}$ per user to reflect individualized trade-offs, such as favoring cost-efficiency or output diversity over raw model quality. These weights are normalized within each dataset to prevent scale bias.

Table 7: Synthetic user weights for MT-Bench dataset.

User	w_{rating}	w_{tokens}	w_{diff}	w_{cost}
user_1	1.42	0.0087	-0.174	-45.23
user_2	1.87	0.0012	0.091	-15.55
user_3	0.96	0.0135	0.045	-48.42
user_4	1.15	-0.0008	-0.220	-10.00
user_5	1.69	0.0024	0.175	-38.50
user_6	1.08	-0.0015	-0.030	-25.12
user_7	0.53	0.0162	0.230	-5.75
user_8	1.34	-0.0005	-0.145	-12.40
user_9	1.98	0.0101	0.087	-25.10
user_10	1.57	0.0024	-0.065	-7.79

B.3 PROCESSING OF THE LAMP DATASET

We select the "Personalized Scholarly Title Generation" task from the LaMP benchmark (Salemi et al., 2024b) as our new dataset. This task provides pairs of paper titles and abstracts for multiple users and requires predicting the title a user would prefer given an abstract.

972
973
974
975
976
977
978
979
980
981
982
983
984
985
986
987
988
989
990
991
992
993
994
995
996
997
998
999
1000
1001
1002
1003
1004
1005
1006
1007
1008
1009
1010
1011
1012
1013
1014
1015
1016
1017
1018
1019
1020
1021
1022
1023
1024
1025
Table 8: **Synthetic user weights for GSM8K dataset.**

User	w_{rating}	w_{tokens}	w_{diff}	w_{cost}
user_1	1.0	20.0	100.0	-0.0
user_2	1.5	18.0	50.0	-1.0
user_3	0.8	22.0	80.0	-0.5
user_4	1.2	17.0	120.0	-0.2
user_5	2.0	15.0	70.0	-0.4
user_6	0.4	6.0	-4.0	-1.0
user_7	0.3	7.0	-5.0	-0.9
user_8	0.6	8.0	-7.0	-1.2
user_9	0.2	9.0	-9.0	-0.8
user_10	0.8	10.0	-3.0	-1.1

Table 9: **Synthetic user weights for MMLU dataset.**

User	w_{rating}	w_{tokens}	w_{diff}	w_{cost}
user_1	1.0	0.00	0.00	0.0
user_2	1.0	0.00	0.00	-600.0
user_3	1.0	0.00	0.00	-1200.0
user_4	1.0	0.00	0.00	-1800.0
user_5	1.0	0.00	0.00	-2400.0

Data extraction. We identify the 10 users with the largest amount of data and randomly sample 200 (title, abstract) pairs for each user.

LLM response generation. We use five LLMs with diverse architectures and sizes—deepseek-r1 (DeepSeek-AI, 2024), gemma-2-27b-it (Team, 2024), llama-3.1-8b-instruct (AI@Meta, 2024), qwen2-7b-instruct (qwe, 2024), and mistral-7b-instruct-v0.3 (Jiang et al., 2023)—to generate a predicted title for each abstract.

User rating acquisition. For each paper, we encode both the ground-truth title and all LLM-generated titles using a PLM. We compute the cosine similarity between a generated title and the ground-truth title and treat this score as the user rating.

Dataset filtering and splitting. For each abstract, we identify the LLM with the highest user rating and use it as the routing target, discarding samples where ties occur. This yields a total of 9,850 instances, which we split into training, validation, and test sets using a 7:1:2 ratio.

C BASELINE ROUTING PROMPTS

To benchmark routing strategies, we design two representative prompt templates: one for a vanilla router that selects the best LLM without personalization, and another for a personalized router that incorporates user history and preferences. Both prompts simulate realistic routing scenarios where a system must choose a single LLM for the next turn in a multi-turn dialogue.

D ADDITIONAL RESULTS FOR CASE STUDIES

D.1 GENERALIZATION

Here, we present the results of the experiments described in Section 5.2 on the ChatBot Arena and MT-Bench datasets, as shown in Figures 6 and 7 respectively.

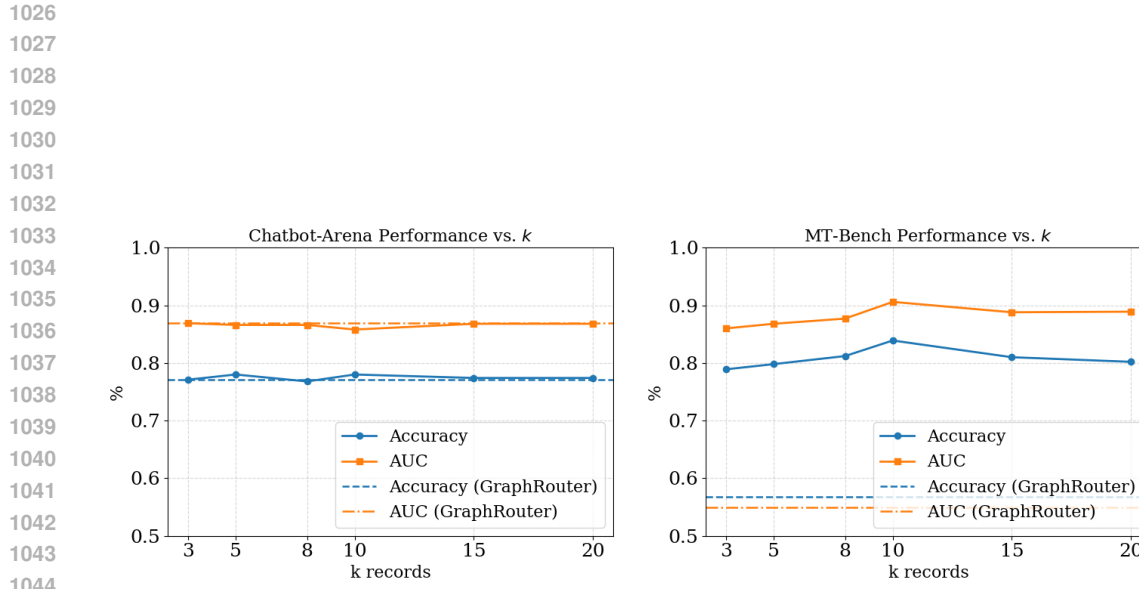


Figure 6: K-selection across datasets.

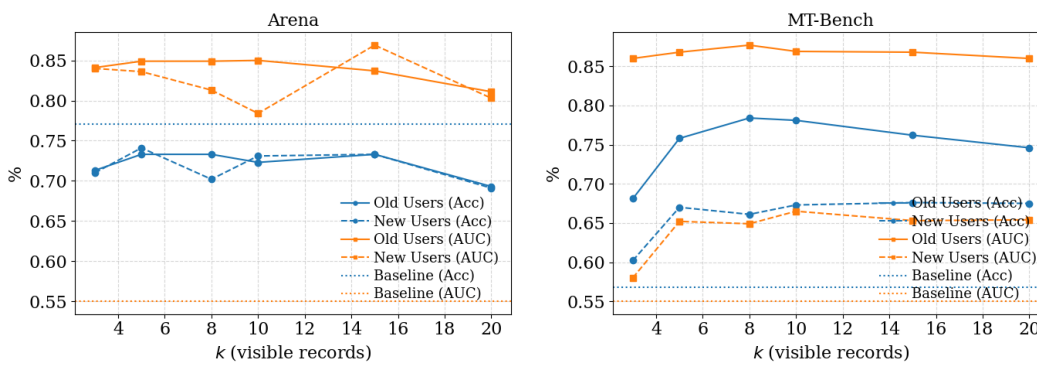


Figure 7: Generalization to new users.

1080
1081
1082 **Table 10: Prompt Template: Vanilla LLM Routing (No Personalization)**
1083
1084
1085
1086
1087
1088
1089
1090
1091
1092
1093
1094
1095
1096
1097
1098
1099
1100**[Instruction]**

You are an expert routing agent. Your task is to select the most suitable Large Language Model (LLM) to handle the next query in a multi-turn conversation.

[Input Format]

[Candidate LLM List]
 {{CANDIDATE_LLM_LIST}}
 [Previous Conversation]
 {{PREVIOUS_CONVERSATION}}
 [Current Query]
 {{CURRENT_QUERY}}

[Instructions for Model Selection]

- Consider the query difficulty, the context of the previous conversation, and each LLM’s expertise, cost, and size.
- Choose the single best LLM to respond to the current query.
- Output only the name of the selected LLM in the exact format below.
- Do not provide explanations or commentary.

[Output Format]

<'{selected_model_name}'>

1101
1102 **Table 11: Prompt Template: Personalized Routing (User History Aware)**
1103**[Instruction]**

You are an expert routing agent. Your task is to select the most suitable Large Language Model (LLM) to handle the next query in a multi-turn conversation, incorporating both model characteristics and personalization signals from the user’s history.

[Input Format]

[Candidate LLM List]
 {{CANDIDATE_LLM_LIST}}
 [Previous Conversation]
 {{PREVIOUS_CONVERSATION}}
 [Current Query]
 {{CURRENT_QUERY}}
 [User Preference History]
 {{USER_PREFERENCE_HISTORY}}

[Instructions for Model Selection]

- Consider the query difficulty, the context of the ongoing conversation, the LLMs’ specializations, cost, and size.
- Additionally, factor in the user’s historical preferences and ratings to personalize the routing decision.
- Choose the single best LLM to respond to the current query.
- Output only the name of the selected LLM in the exact format below.
- Do not provide explanations or commentary.

[Output Format]

<'{selected_model_name}'>

1128
1129
1130 **E THE USE OF LARGE LANGUAGE MODELS (LLMs)**
11311132
1133 During the writing of this paper, we used the GPT-5 Mini model for text polishing and grammatical corrections to enhance the readability of the manuscript.

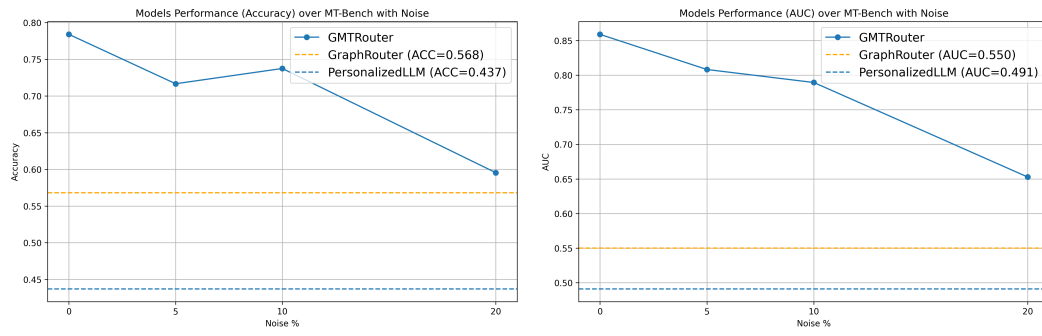


Figure 8: Performance against noisy preference over MT-Bench

F FURTHER EXPERIMENT

F.1 EXTENDED EXPERIMENTS ON CHATBOT ARENA USERS

Table 12: GMTRouter performance on the ChatBot Arena dataset with newly added users.

	New Users = 0	New Users = 3	New Users = 161
Accuracy	0.774	0.780	0.790
AUC-ROC	0.875	0.858	0.837

To more thoroughly validate that GMTRouter exhibits strong generalization to new users, we further selected all ChatBot Arena users with more than 15 historical interactions (161 users in total). We keep the original training and test sets used in Section 5 unchanged and use all newly added data exclusively as the test set. GMTRouter is then evaluated on these newly added users. The experimental results are shown in Table 12.

This expanded evaluation enables us to assess GMTRouter on a substantially larger user set and further demonstrates its effectiveness and generalization capability.

F.2 EXPERIMENTS WITH NOISY DATA

We conduct experiments to evaluate GMTRouter’s personalization performance under varying levels of noisy data. Specifically, we use the MT-Bench dataset and swap the user ratings of $k\%$ of the data ($k = 5, 10, 20$), simulating noise and inconsistencies in preference signals (Li et al., 2024a). The experimental results are shown in Figure 8. Our results indicate that, although performance naturally decreases as noise increases, GMTRouter **degrades gracefully and remains competitive even with 20% noise, outperforming the strongest baseline trained on clean data**. We attribute this robustness to **user-conditioned graph sampling**, which aggregates signals across multiple interactions and mitigates the impact of individual noisy labels.

F.3 COMPARISON WITH PERSONALIZED GENERATION METHOD

To evaluate the personalization capabilities of GMTRouter against personalized generation approaches, we adopt the untuned In-Prompt Augmentation (IPA) based Retrieval Augmented Generation (RAG) from the LaMP benchmark (Salemi et al., 2024b), employing Contriever (Izacard et al., 2021) as the retrieval backbone.

Experiments were conducted on the LaMP dataset. For the RAG baseline, we utilized the test set’s ‘abstract’ query to retrieve the **top-10** most relevant historical ‘abstracts’ from the specific user’s training data. These retrieved items were formatted as ‘title, abstract’ pairs and integrated into the LLM’s input as few-shot examples. Crucially, while GMTRouter relies on user ratings (calculated by comparing the LLM’s predicted titles against the ground-truth titles) as its supervision signal,

1188 we provided the RAG baseline with a **more direct and potent** form of supervision by explicitly
 1189 incorporating the retrieved ground-truth titles into the few-shot examples.
 1190

1191 We employ **average user rating** and **average token usage** as our primary evaluation metrics. The
 1192 GMTRouter output consists of the raw response generated by the routed LLM, whereas the RAG
 1193 output is generated by DeepSeek-R1 (DeepSeek-AI, 2024), conditioned on the prompt augmented
 1194 with the retrieved few-shot examples. Furthermore, we also investigated the personalization capa-
 1195 bilities of combining both GMTRouter and RAG. Specifically, GMTRouter is employed to select
 1196 the optimal LLM, and the RAG is subsequently used to construct the few-shot augmented prompt.
 1197 The experimental results are presented in Table 13.
 1198

1198 Table 13: Performance Comparison of GMTRouter and IPA-RAG on the LaMP Benchmark. The **Random**
 1199 **Routing** column serves as the **lower bound**, representing the expected user rating achieved by randomly select-
 1200 ing an LLM. Conversely, the **Theoretical Best Routing** column establishes the **upper bound** for the routing
 1201 task, reflecting the user rating obtained by always selecting the LLM that yields the highest user rating for that
 1202 specific instance.

Metric	Random Routing	GMTRouter	IPA-RAG	GMTRouter + IPA-RAG	Theoretical Best Routing
AVG User Rating	0.744	0.772	0.775	0.784	0.810
AVG Token Cost	–	293.56	3231.72	2358.89	–

1206 Our experiments lead to three key observations:
 1207

1. **Comparable Personalization:** Both GMTRouter (routing) and the personalized genera-
 1209 tion approach (IPA-RAG) achieve comparable improvements in personalization capability
 1210 as measured by the AVG User Rating.
2. **Cost Disparity:** The IPA-RAG baseline incurs a significantly higher cost, requiring several
 1212 times more tokens than GMTRouter, highlighting the efficiency gains offered by the routing
 1213 mechanism.
3. **Synergistic Effect:** Combining the two methods (GMTRouter + IPA-RAG) yields the best
 1215 empirical performance. This suggests that routing and personalized generation techniques
 1216 address distinct, complementary facets of personalization.

1218 Table 14: GMTRouter performance using different heterogeneous convolutional layers.
 1219

Conv Layer	Chatbot-Arena	MT-Bench	GSM8K	MMLU
	ACC / AUC	ACC / AUC	ACC / AUC	ACC / AUC
HeteroConv	0.777 / 0.867	0.569 / 0.492	0.499 / 0.603	0.494 / 0.542
HANConv	0.766 / 0.776	0.646 / 0.680	0.774 / 0.775	0.707 / 0.746
HGTConv	0.774 / 0.875	0.784 / 0.859	0.773 / 0.859	0.771 / 0.870

1228 F.4 USING DIFFERENT HETEROGENEOUS GNNS AS THE GMTRROUTER BACKBONE

1229 We investigate how different heterogeneous GNNS used as the GMTRouter backbone affect its per-
 1230 sonalization capability. We evaluate three backbones: HGT (Ziniu Hu, 2020), HAN Wang et al.
 1231 (2019), and HeteroConv, and present the results in Table 14.
 1232

1233 We observe that attention-based heterogeneous GNNS (HAN, HGT) consistently outperform the
 1234 simpler aggregation-based HeteroConv backbone. These results also indicate that GMTRouter is not
 1235 dependent on any particular GNN architecture: multiple attention-based backbones achieve strong
 1236 performance, suggesting that the improvements mainly stem from the graph-based personalized
 1237 routing framework and data modeling, rather than from a specific convolutional operator.
 1238